J|A|C|S
ARTICLES
Published on Web 10/05/2004

Amplified Quenching of a Conjugated Polyelectrolyte by Cyanine Dyes

Chunyan Tan, Evrim Atas, Jürgen G. Müller, Mauricio R. Pinto, Valeria D. Kleiman,* and Kirk S. Schanze*

Contribution from the Department of Chemistry, University of Florida, Gainesville, Florida 32611-7200

Received May 27, 2004; E-mail: kschanze@chem.ufl.edu; kleiman@chem.ufl.edu

Abstract: The conjugated polyelectrolyte PPESO3 features a poly(phenylene ethynylene) backbone substituted with anionic 3-sulfonatopropyloxy groups. PPESO3 is quenched very efficiently ($K_{SV} > 10^6$ M^{-1}) by cationic energy transfer quenchers in an amplified quenching process. In the present investigation, steady-state and picosecond time-resolved fluorescence spectroscopy are used to examine amplified quenching of PPESO3 by a series of cyanine dyes via singlet−singlet energy transfer. The goal of this work is to understand the mechanism of amplified quenching and to characterize important parameters that govern the amplification process. Steady-state fluorescence quenching of PPESO3 by three cationic oxacarbocyanine dyes in methanol solution shows that the quenching efficiency does not correlate with the Förster radius computed from spectral overlap of the PPESO3 fluorescence with the cyanines' absorption. The quenching efficiency is controlled by the stability of the polymer−dye association complex. When quenching studies are carried out in water where PPESO3 is aggregated, changes observed in the absorption and fluorescence spectra of 1,1′,3,3,3′,3′-hexamethylindotricarbocyanine iodide (HMIDC) indicate that the polymer templates the formation of a J-aggregate of the dye. The fluorescence dynamics in the PPESO3/HMIDC system were probed by time-resolved upconversion and the results show that PPESO3 to HMIDC energy transfer occurs on two distinctive time scales. At low HMIDC concentration, the dynamics are dominated by an energy transfer pathway with a time scale faster than 4 ps. With increasing HMIDC concentration, an energy pathway with a time scale of 0.1−1 ns is active. The prompt pathway ($\tau < 4$ ps) is attributed to quenching of delocalized PPESO3 excitons created near the HMIDC association site, whereas the slow phase is attributed to intra- and interchain exciton diffusion to the HMIDC.

Introduction

Conjugated polyelectrolytes (CPEs) are π-conjugated polymers that feature ionic solubilizing side groups.[1] These materials show many of the interesting and useful properties exhibited by π-conjugated polymers, namely, strong light absorption, strong fluorescence, electroactivity, and good transport properties for charge carriers and excitons.[2−7] In addition, CPEs are typically soluble in water and other polar solvents, and consequently they can be processed into films and other supramolecular assemblies from aqueous solution.[6−11]

Interaction of CPEs with aqueous soluble species such as metal ions,[12] organic ions,[4,10,13−17] biomolecules,[4,15,18] and biopolymers[19,20] has been a subject of considerable interest. In this regard, it has been found that many ionic species quench the fluorescence of oppositely charged CPEs with extremely high sensitivity.[4,10,12−18] This effect has been termed "amplified quenching"[21] or "superquenching".[15] The amplified quenching effect has been demonstrated to arise with quenchers that operate by either electron or energy transfer. In some cases, Stern−

(1) For a recent review of the synthesis, properties, and applications of CPEs, see Pinto, M. R.; Schanze, K. S. *Synthesis—Stuttgart* **2002**, 1293−1309.
(2) Patil, A. O.; Ikenoue, Y.; Wudl, F.; Heeger, A. J. *J. Am. Chem. Soc.* **1987**, *109*, 1858−1859.
(3) Shi, S.; Wudl, F. *J. Am. Chem. Soc.* **1990**, *23*, 2119−2124.
(4) Chen, L.; McBranch, D. W.; Wang, H.-L.; Helgeson, R.; Wudl, F.; Whitten, D. G. *Proc. Natl. Acad. Sci. U.S.A.* **1999**, *96*, 12287−12292.
(5) Tan, C.; Pinto, M. R.; Schanze, K. S. *Chem. Commun.* **2002**, 446−447.
(6) Lukkari, J.; Salomaki, M.; Viinikanoja, A.; Aaritalo, T.; Paukkunene, J.; Kocharova, N.; Kankare, J. *J. Am. Chem. Soc.* **2001**, *123*, 6083−6091.
(7) Cutler, C. A.; Bouguettaya, M.; Reynolds, J. R. *Adv. Mater.* **2002**, *14*, 684−688.
(8) McQuade, D. T.; Swager, T. M. *J. Am. Chem. Soc.* **2000**, *122*, 12389−12390.
(9) Jones, R. M.; Bergstedt, T. S.; McBranch, D. W.; Whitten, D. G. *J. Am. Chem. Soc.* **2001**, *123*, 6726−6727.
(10) Pinto, M. R.; Kristal, B. M.; Schanze, K. S. *Langmuir* **2003**, *19*, 6523−6533.
(11) Thunemann, A. F. *Langmuir* **2001**, *17*, 5098−5102.
(12) Harrison, B. S.; Ramey, M. B.; Reynolds, J. R.; Schanze, K. S. *J. Am. Chem. Soc.* **2000**, *122*, 8561−8562.
(13) Chen, L. H.; McBranch, D.; Wang, R.; Whitten, D. *Chem. Phys. Lett.* **2000**, *330*, 27−33.
(14) Chen, L. H.; Xu, S.; McBranch, D.; Whitten, D. *J. Am. Chem. Soc.* **2000**, *122*, 9302−9303.
(15) Whitten, D.; Chen, L.; Jones, R.; Bergstedt, T.; Heeger, P.; McBranch, D. In *Optical Sensors and Switches*; Ramamurthy, V., Schanze, K. S., Eds.; Marcel Dekker: New York, 2001; pp 189−208.
(16) Wang, J.; Wang, D. L.; Miller, E. K.; Moses, D.; Bazan, G. C.; Heeger, A. J. *Macromolecules* **2000**, *33*, 5153−5158.
(17) Wang, D. L.; Wang, J.; Moses, D.; Bazan, G. C.; Heeger, A. J.; Park, J. H.; Park, Y. W. *Synth. Met.* **2001**, *119*, 587−588.
(18) Kushon, S. A.; Ley, K. D.; Bradford, K.; Jones, R. M.; McBranch, D.; Whitten, D. *Langmuir* **2002**, *18*, 7245−7249.
(19) Fan, C.; Plaxco, K. W.; Heeger, A. J. *J. Am. Chem. Soc.* **2002**, *124*, 5642−5643.
(20) Gaylord, B. S.; Heeger, A. J.; Bazan, G. C. *J. Am. Chem. Soc.* **2003**, *125*, 896−900.
(21) Zhou, Q.; Swager, T. M. *J. Am. Chem. Soc.* **1995**, *117*, 12593−12602.

Scheme 1

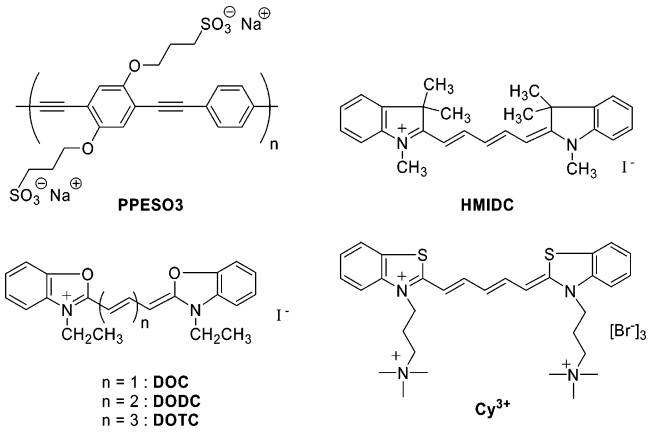

Volmer (SV) quenching constants (K_{SV}) as large as 10^8 M^{-1} have been reported.[12,22] The amplified quenching effect has been attributed to at least two features unique to the CPE−ionic quencher systems, namely, ion pairing between CPE chains and the oppositely charged quencher species and ultrafast intrachain diffusion of the exciton within the CPE.[4,12] There is also strong evidence that the CPE aggregates in aqueous solution and the amplified quenching effect is enhanced further in the aggregate.[4,5,10,14] This observation suggests that interchain exciton diffusion may also play a role in amplified quenching. Although the mechanism of amplified quenching has not been probed in great detail, the effect has already been harnessed to develop a new family of fluorescence-based sensors for biological targets such as small biomolecules, proteins, and nucleic acids.[4,15,18,20,23−27]

We have an interest in developing a fundamental understanding of the mechanism of amplified quenching in CPE−ionic quencher systems. In particular, we are interested in understanding the mechanism and dynamics of exciton diffusion within CPE single chains and how it influences the overall efficiency of amplified quenching. To address this issue, we carried out a detailed photophysical investigation that probes the interaction of the sulfonate-substituted poly(phenylene ethynylene) PPESO3 with a series of cationic cyanine dyes (structures in Scheme 1). PPESO3 is a water- and alcohol-soluble polymer that exhibits a strong blue or green fluorescence.[5] Cyanine dyes were selected for this investigation for several reasons. First, cyanines are cationic and therefore interact with PPESO3 by ion pairing. Second, cyanines absorb and fluoresce strongly, and their absorption and fluorescence wavelengths can be tuned systematically by subtle structural modification.[28] Finally, because cyanines absorb strongly in the visible region, they efficiently quench the fluorescence of anionic CPEs, and the quenching mechanism is believed to be energy transfer from the polymer to the dye. In the present study we probe in detail the mechanism by which cyanines quench PPESO3 by using optical absorption and steady-state and picosecond time-resolved fluorescence spectroscopy. The results clearly indicate that amplified quenching occurs via energy transfer from PPESO3 to the dye acceptor. Time-resolved fluorescence results also demonstrate that at very low quencher:polymer repeat unit (PRU) ratios a large fraction of the energy transfer is completed within a few picoseconds. The results imply that amplified quenching is significantly enhanced by the strongly delocalized singlet exciton in the poly(phenylene ethynylene) chains and aggregates.

Experimental Section

Materials. The synthesis and characterization of PPESO3 was previously described.[5] The polymer was purified by dialysis against deionized water, and it was stored as an aqueous stock solution in the dark under an argon atmosphere. The number-averaged molecular weight (M_n) of PPESO3 is estimated as 100 000 on the basis of ultrafiltration and end-group analysis. Viscometry of PPESO3 in 0.1 LiBr/dimtheyl sulfoxide (DMSO) solution yields an intrinsic viscosity of $[\eta] = 3.84$ dL·g^{-1} (see Supporting Information). By using the Mark−Houwink relation, $[\eta] = KM_v^a$ (where K and a are empirically determined constants and M_v is the viscosity-averaged molecular weight),[29] it is possible to estimate the M_v value of PPESO3 by using K and a values for a structurally related polyelectrolyte. By using $K = 1.46 \times 10^{-4}$ dL·g^{-1} and $a = 0.8$ [obtained for poly(sodium acrylate) in 0.1 M NaCl],[30] we obtain $M_v = 330\,000$ g·mol^{-1} for PPESO3.

The extinction coefficient of PPESO3 was determined in methanol by gravimetric analysis and it is $\epsilon = 57\,000$ M^{-1} cm^{-1} (all concentrations are provided as polymer repeat unit concentration, [PRU]). The polymer stock solution concentration was 2.08 mg·mL^{-1}, which corresponds to [PRU] = 4 mM. The stock solution was diluted as needed to prepare solutions used for spectroscopic experiments. Final concentrations of the diluted PPESO3 solutions were determined on the basis of the polymer's extinction coefficient. The cyanine dyes HMIDC, DOC, DODC, DOTC, and Cy^{3+} (Scheme 1) were obtained from Aldrich Chemical, Fisher Scientific, or Molecular Probes and they were used as received. The purity of the dyes was confirmed by NMR spectroscopy. Cyanine stock solutions were prepared in methanol. The water used in all experiments was prepared in a Millipore Milli-Q plus purification system and displayed a resistivity of ≥18.2 MΩ·cm^{-1}. The methanol used in all experiments was commercial HPLC-grade.

Concentration-Dependent Steady-State Fluorescence and Absorption Spectroscopy. Fluorescence quenching and absorption experiments were carried out by microtitration in a fluorescence cuvette. In a typical titration quenching experiment, 2 mL of a PPESO3 (or cyanine) solution was placed in a 1 cm quartz fluorescence cell. The UV−visible absorption and fluorescence spectra were recorded at room temperature. Then absorption and/or fluorescence spectra were repeatedly acquired after the addition of microliter aliquots of a concentrated solution that contained the cyanine dye quencher (or the polymer in the case of polymer addition experiments). Dye (and polymer) solution aliquots were delivered by use of a calibrated Eppendorf microliter pipet.

Instrumentation. Absorption spectra were obtained on a Varian-Cary 100 UV−visible absorption spectrometer. Steady-state photoluminescence spectroscopy was carried out on a SPEX Fluorog instrument. Emission spectra were corrected by using correction factors generated in-house with a standard calibration lamp.

(22) Wang, D. L.; Wang, J.; Moses, D.; Bazan, G. C.; Heeger, A. J. *Langmuir* **2001**, *17*, 1262−1266.
(23) Gaylord, B. S.; Heeger, A. J.; Bazan, G. C. *Proc. Natl. Acad. Sci. U.S.A.* **2002**, *99*, 10954−10957.
(24) Wilson, J. N.; Wang, Y.; Lavigne, J. J.; Bunz, U. H. F. *Chem. Commun.* **2003**, 1626−1627.
(25) Dore, K.; Dubus, S.; Ho, H. A.; Levesque, I.; Brunette, M.; Corbeil, G.; Boissinot, M.; Boivin, G.; Bergeron, M. G.; Boudreau, D.; Leclerc, M. *J. Am. Chem. Soc.* **2004**, *126*, 4240−4244.
(26) Pinto, M. R.; Schanze, K. S. *Proc. Natl. Acad. Sci. U.S.A.* **2004**, 7505−7510.
(27) Kumaraswamy, S.; Bergstedt, T.; Shi, X.; Rininsland, F.; Kushon, S.; Xia, W.; Ley, K.; Achyuthan, K.; McBranch, D.; Whitten, D. *Proc. Natl. Acad. Sci. U.S.A.* **2004**, *101*, 7511−7515.
(28) Sturmer, D. M. *Synthesis and Properties of Cynanine Dyes and Related Dyes*; Wiley: New York, 1977; Vol. 30.
(29) van Krevelen, D. W. *Properties of Polymers, Their Estimation and Correlation with Chemical Structure*; Elsevier Scientific Publishing: New York, 1976.
(30) Kato, T.; Tokuya, T.; Nozaki, T.; Takahashi, A. *Polymer* **1984**, *25*, 218−224.

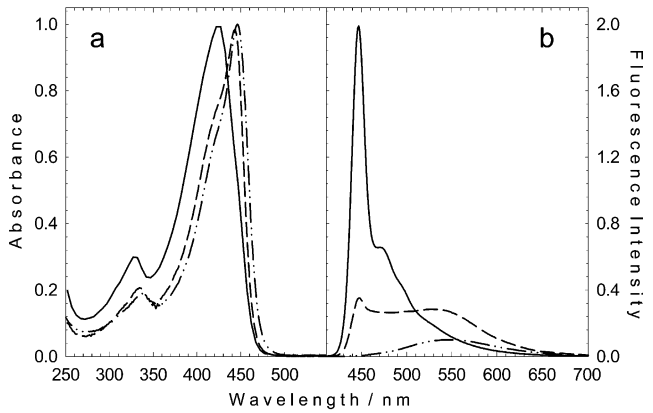

Figure 1. UV−visible absorption (a) and fluorescence emission spectra (b) of PPESO3 in CH_3OH (—), 1:1 CH_3OH/H_2O (− − −), and H_2O (− ·· −). Fluorescence emission spectra were measured with excitation wavelength at 400 nm and are normalized to reflect relative quantum yields.

Time-resolved fluorescence experiments were carried out by fluorescence upconversion.[31] The upconversion experiment allows one to measure the temporal evolution of the sample fluorescence by sum-frequency generation of the emission with an ultrafast gate pulse in a nonlinear crystal.[31] The excitation pulses were produced by harmonic generation of the output of an optical parametric amplifier (OPA) pumped by a laser system consisting of a Ti:sapphire oscillator (Spectra Physics) and a regenerative Ti:sapphire amplifier (Spectra Physics) running at 1 kHz. Pulses shorter than 100 fs (full width at half-maximum, FWHM) are focused on a rotating cell (1 mm path length, 250 μm focal diameter, 100 nJ·pulse^{-1}) containing a solution of polymer and dye in CH_3OH with an optical density of 0.3 at the excitation wavelength. The fluorescence collected by a pair of off-axis parabolic mirrors is overlapped on a nonlinear crystal (β-BBO, type I, 0.5 mm) with a fraction of the Ti:sapphire amplifier output (30 μJ/pulse, 60 fs FWHM) acting as a fast optical shutter. The simultaneous spatial and temporal overlap of the gate and fluorescence in the nonlinear crystal leads to generation of the sum-frequency signal, which is spectrally filtered by a monochromator and detected by a photomultiplier (Hamamatsu R928). By varying the time delay between the short excitation and gate pulses, the ultrafast emission dynamics is mapped out.

Results and Discussion

Photophysics of PPESO3 in Water and Methanol. PPESO3 absorbs in the blue of the visible region and it is strongly fluorescent. As reported in a preliminary communication,[5] the absorption and fluorescence properties of the polymer are solvent-dependent. Because this effect is important to understand the work described herein, a brief summary is provided. Figure 1 illustrates the absorption and fluorescence of PPESO3 in H_2O, 1:1 H_2O/CH_3OH, and CH_3OH. The absorption spectrum of the polymer red-shifts and narrows as the solvent is changed from CH_3OH to H_2O. This feature suggests that the conjugation length and degree of structural order along the backbone increases with the volume fraction of H_2O.

More information regarding the effect of solvent on PPESO3 comes from the fluorescence spectra. Specifically, the fluorescence of the polymer in CH_3OH is a narrow band with only a small shoulder on the long-wavelength side due to electron-vibrational coupling. Importantly, the CH_3OH spectrum is very similar in appearance to the fluorescence spectra of organic-soluble poly(phenylene ethynylene)s (PPEs) in good solvents where the degree of polymer aggregation is minimal.[32−34] With increasing volume fraction of water in the solvent, the characteristic unaggregated PPESO3 emission band disappears and a new broad fluorescence band appears at longer wavelengths. In pure water the fluorescence appears as a broad, structureless band that is red-shifted ~100 nm from the maximum in CH_3OH. In addition, the fluorescence quantum efficiency decreases substantially from CH_3OH to water (from 0.78 to 0.10). The fluorescence spectra clearly indicate that in solutions that contain increasing volume fractions of water, the polymer exists in a strongly aggregated form. The broad, structureless fluorescence spectrum and relatively low fluorescence quantum efficiency that are characteristic of the aggregated state of the polymer likely arise because the emitting state is dominated by an excimer-like[35] structure, which likely involves π-stacking interactions between phenylene rings on adjacent chains stabilized by hydrophobic interaction (Scheme 2). The red-shift in the absorption accompanying the formation of the polymer aggregate in water is believed to arise from π-stacking between adjacent PPE chains, inducing the phenylene rings to adopt an all-planar conformation, effectively increasing intrachain conjugation.[36,37]

In summary, absorption and fluorescence studies suggest that in water PPESO3 exists in a strongly aggregated state, with extensive interchain π-stacking. By contrast, in CH_3OH solution, the polymer is more strongly solvated, and little photophysical evidence exists for the presence of aggregates.

Fluorescence Quenching Mechanisms. Before we present the details of the fluorescence quenching experiments, it is necessary to provide a brief overview of quenching mechanisms and models.[38] Fluorescence quenching can occur by two limiting mechanisms, dynamic

$$F^* + Q \xrightarrow{k_q} F + Q \qquad (1a)$$

and static

$$F + Q \overset{K_a}{\rightleftharpoons} [F,Q] \xrightarrow{h\nu} [F^*,Q] \xrightarrow{\text{fast}} F + Q \qquad (1b)$$

where F* is an excited-state fluorophore, Q is a quencher, k_q is the bimolecular quenching rate constant, and K_a is the association constant for formation of the ground-state complex [F, Q]. Treatment of fluorescence intensity quenching data according to the Stern−Volmer (SV) equation yields

$$\frac{I^0}{I} = 1 + K_{SV}[Q] \qquad (2)$$

where I and I^0 are the fluorescence intensity with and without Q, respectively, and K_{SV} is the SV quenching constant. In the limit where quenching is dominated by the dynamic pathway

(31) Schanz, R.; Kovalenko, S. A.; Kharlanov, V.; Ernsting, N. P. *Appl. Phys. Lett.* **2001**, *79*, 566−568.
(32) Yang, J.-S.; Swager, T. M. *J. Am. Chem. Soc.* **1998**, *120*, 11864−11873.
(33) Huang, W. Y.; Matsuoka, S.; Kwei, T. K.; Okamoto, Y. *Macromolecules* **2001**, *34*, 7166−7171.
(34) Halkyard, C. E.; Rampey, M. E.; Kloppenburg, L.; Studer-Martinez, S. L.; Bunz, U. H. F. *Macromolecules* **1998**, *31*, 8655−8659.
(35) Gordon, M., Ware, W. R., Eds. *The Exciplex*; Academic Press: New York, 1975.
(36) Miteva, T.; Palmer, L.; Kloppenburg, L.; Neher, D.; Bunz, U. H. F. *Macromolecules* **2000**, *33*, 652−654.
(37) Kim, J.; Swager, T. M. *Nature* **2001**, *411*, 1030−1034.
(38) Lakowicz, J. R. *Principles of Fluorescence Spectroscopy*, 2nd ed.; Kluwer Academic/Plenum Publishers: New York, 1999.

Scheme 2

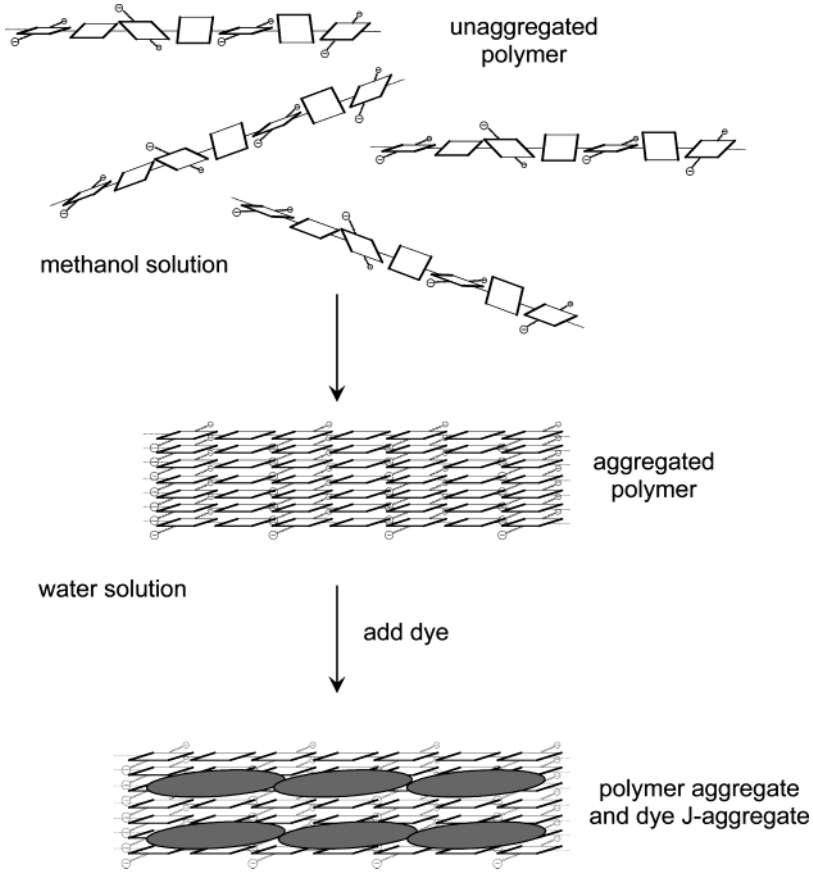

(eq 1a), $K_{SV} = k_q\tau^0$, where τ^0 is the fluorescence lifetime of F*, whereas in the limit where static quenching dominates, $K_{SV} = K_a$.

There are several ways to distinguish between dynamic and static quenching. First, note that k_q cannot exceed the diffusion rate constant (ca. 10^{10} M^{-1} s^{-1}) when quenching is fully dynamic. Since $K_{SV} = k_q\tau^0$, for a fluorophore that has a 1 ns lifetime this places an upper limit on $K_{SV} \approx 10$ M^{-1}. Thus, static quenching may be important if the experimentally observed K_{SV} is significantly greater than 10 M^{-1}. Another method for distinguishing when static quenching is important is to compare the ratio of emission lifetimes (τ^0/τ) and emission intensities (I^0/I) vs quencher concentration. If the K_{SV} obtained from intensity quenching is greater than that from lifetime quenching, then static quenching is occurring.

When the quenching is dominated by either a purely static or a dynamic pathway, the quenching behavior follows eq 2 and consequently SV plots of I^0/I vs [Q] are linear. However, in many situations (as shown below) the SV plots are curved upward. Curvature in the SV plots can arise from a variety of processes, including mixed static and dynamic quenching, variation in the association constant with quencher concentration, and chromophore (or polymer) aggregation. Although a number of quantitative models have been used to fit nonlinear SV plots observed in the quenching of conjugated polyelectrolytes,[16,22,39] due to the complexity of the polymer−quencher systems that are the focus of the present investigation (i.e., quencher-induced polymer aggregation, vide infra), we are reluctant to apply these models in the present investigation. Therefore, to provide a semiempirical measure of the magnitude of the quenching in the various PPESO3−dye systems, we discuss the quenching in terms of K_{SV} values computed by linear fits of the SV plots at low quencher concentrations where the plots are nearly linear, as well as the quencher concentration required to quench 90% of the polymer's fluorescence ($[Q]_{90}$). Note that more efficient quenching is signaled by larger K_{SV} and smaller $[Q]_{90}$ values.

Steady-State Fluorescence Quenching of PPESO3 by Cyanines in Methanol. As shown in detail below, cyanine dyes quench the fluorescence of PPESO3 via singlet−singlet energy transfer, where PPESO3 is the donor and the cyanine dye is the acceptor:

$$^1\text{PPESO3}^* + \text{cyanine} \rightarrow \text{PPESO3} + {}^1\text{cyanine}^* \quad (3)$$

In every case examined, the occurrence of singlet−singlet energy transfer is confirmed by the observation of sensitized fluorescence from the cyanine dye acceptor concomitant with quenching of the polymer's fluorescence (examples shown below).

In experiments designed to explore whether Förster energy transfer theory[40] could be used to correlate the relative quenching efficiency of the cyanine dyes, quenching of PPESO3 by the series of cyanines DOC, DODC, and DOTC (Scheme 1) was investigated. These experiments were carried out in CH_3OH solution to minimize possible complications arising from polymer aggregation. DOC, DODC, and DOTC comprise a homologous series of dyes that differ only in the conjugation length of the merocyanine linker chain. As shown in Table 1,

(39) Murphy, C. B.; Zhang, Y.; Troxler, T.; Ferry, V.; Martin, J. J.; Jones, W. E., Jr. *J. Phys. Chem. B* **2004**, *108*, 1537−1543.

(40) Förster, T. *Faraday Discuss.* **1959**, *27*, 7−17.

Table 1. Photophysics and Quenching of PPESO3 with Cyanine Dyes in Methanol[a]

dye	λ_{max}^{abs}/nm (ϵ_{max}/M^{-1} cm^{-1})	λ_{max}^{em}/nm	ϕ_{fl}	Förster radius R_0/Å	K_{SV} [b]/M^{-1}	$[Q]_{90}$[c]/μM
PPESO3	425 (57 000)[5]	450	0.78[5]			
DOC	483 (140 000)[41]	503	0.04[42]	59	4.6×10^5	>5
DODC	582 (238 000)[43]	614	0.49[44]	56	5.8×10^5	4.8
DOTC	678 (250 000)[41]	713	0.49[45]	49	1.3×10^6	2.2
HMIDC	636 (230 000)[46]	663	0.18[46]	50	1.1×10^6	≈4
Cy^{3+}	647 (166 000)[47]	682	0.27[46]	47	1.0×10^6	1.4

[a] Citations in table provide source of data. [b] Computed from linear fit at low quencher concentration. [c] Quencher concentration at 90% quenching (i.e., $I^0/I = 10$).

the wavelengths of the absorption and fluorescence maxima systematically increase in the sequence DOC < DODC < DOTC. (Figure S2 in Supporting Information shows the PPESO3 fluorescence along with the absorption of the three cyanines.) As a consequence of this red-shift in dye absorption and fluorescence, spectral overlap between the absorption of the cyanine acceptor and the emission of the PPESO3 donor varies systematically. By use of Förster theory it is possible to compute the Förster radius, R_0, which provides a relative measure of the dipole−dipole coupling between an energy donor and acceptor.[38,40] Table 1 contains the computed R_0 values for the cyanine dyes.[48] As expected, the R_0 values vary in the sequence DOC > DODC > DOTC.[49]

Figure 2a illustrates the SV quenching plots for PPESO3 (10 μM) in CH_3OH by DOC, DODC, and DOTC. In each case the SV plots are curved upward, and consequently we characterize the plots using K_{SV} values computed at low quencher concentration and $[Q]_{90}$ values. The K_{SV} and $[Q]_{90}$ values are listed in Table 1. The three dyes quench PPESO3 fluorescence very efficiently: for example, at a concentration of 1 μM, DOTC quenches PPESO3 fluorescence by 75%. The K_{SV} values vary from $\sim 4.6 \times 10^5$ M^{-1} (DOC) to $\sim 1.3 \times 10^6$ M^{-1} (DOTC), and the $[Q]_{90}$ values range from >5 μM (DOC) to 2.2 μM (DOTC). Given that the fluorescence lifetime of PPESO3 in CH_3OH is 150 ps (see below), the maximum K_{SV} expected for a dynamic quenching would be ~ 1.5 M^{-1}. The highly efficient quenching cannot be accounted for by a diffusion-controlled process. Association of the cationic dye quenchers with the anionic polymer chain must be involved in the quenching mechanism.

The overall efficiency by which the three dyes quench PPESO3 fluorescence runs counter to expectation on the basis of Förster theory. In particular, although DOC has the largest

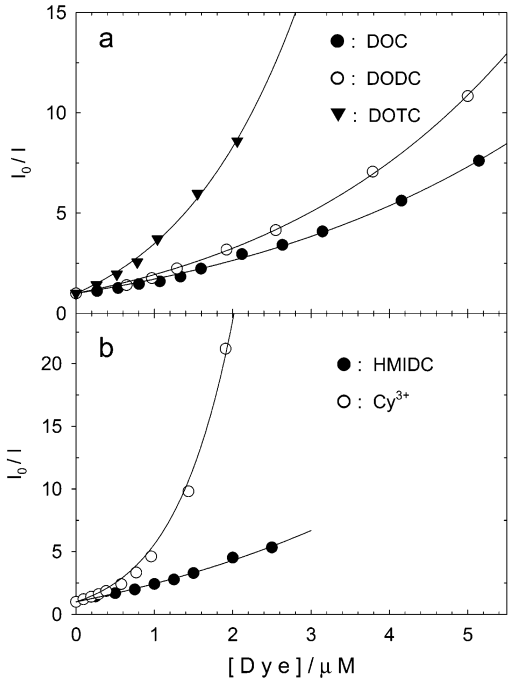

Figure 2. Stern−Volmer plots of PPESO3 (10 μM) fluorescence quenched by cyanine dyes in CH_3OH. (a) Three oxocarbocyanine dye-quenchers: DOC (●), DODC (○), and DOTC (▼); (b) HMIDC (●) and Cy^{3+} (○). (Lines are drawn through the plots to aid the eye.)

Förster R_0, it is the least efficient quencher (smallest K_{sv} and largest $[Q]_{90}$ values, see Table 1). By contrast, DOTC has the smallest R_0, whereas it is the most efficient quencher. These results clearly indicate that a factor other than the efficiency of Förster dipole−dipole coupling determines the efficiency by which the cyanines quench the polymer's fluorescence. We suggest that the overall observed quenching efficiency is determined by the association constant (K_a) for binding of the cyanines to PPESO3 (i.e., the system is in the static quenching limit, where $K_{SV} = K_a$). Thus, the difference in quenching efficiency among the three cyanines reflects differences in association constants for the dye−polymer complexes. While the polymer−dye electrostatic interaction is likely to be what drives the association, solvophobic and $\pi-\pi$ interactions are also likely to play a role in stabilizing the complexes. We believe that the latter two terms explain the fact that DOTC, the largest dye, is the most efficient quencher. Within this model it is implicit that the quenching is dominated by a static mechanism, whereby quenching is virtually instantaneous for a significant fraction of the excitons produced on a polymer chain complexed to a dye quencher. This concept is supported by the results of ultrafast time-resolved fluorescence spectroscopy that are presented below.

(41) Sims, P. J.; Waggoner, A. S.; Wang, C. H.; Hoffman, J. F. *Biochemistry* **1974**, *13*, 3315−3330.
(42) O'Brien, D. F.; Kelly, T. M.; Costa, L. F. *Photogr. Sci. Eng.* **1974**, *18*, 76−84.
(43) Tredwell, C. J.; Keary, C. M. *Chem. Phys.* **1979**, *43*, 307−316.
(44) Dempster, D. N.; Thompson, G. F.; Morrow, T.; Rankin, R. *J. Chem. Soc. Faraday 2* **1972**, *68*, 1479ff.
(45) Birge, R. R. *Kodak Laser Dyes*, 1987.
(46) Haughland, R. P. *Handbook of Fluorescent Probes and Research Products*; Molecular Probes, Inc.: Eugene, OR, 2002.
(47) Wang, M. M.; Silva, G. L.; Armitage, B. A. *J. Am. Chem. Soc.* **2000**, *122*, 9977−9986.
(48) $R_0 = 0.211[\kappa^2 n^{-4} \phi_D J(\lambda)]^{1/6}$, where κ accounts for the relative orientation of the transition dipoles of the two chromophores ($\kappa^2 = {}^2/_3$ for randomly oriented dipoles), ϕ_D is the fluorescence quantum yield of the donor (0.78 for PPESO3 in MeOH), n is the solvent refractive index, and $J(\lambda)$ is the donor−acceptor spectral overlap integral.
(49) The difference in R_0 values between DOC and DODC is not as great as might be expected simply on the basis of the red-shift in the absorption maximum of the DODC relative to DOC. The less-than-expected decrease in R_0 arises because the oscillator strength of the cyanine dye absorption increases with conjugation length (see Table 1) and this effect partially compensates for the decreased wavelength matching of the polymer's fluorescence with the dyes' absorption bands.

To further test the concept that the polymer−dye association plays a predominant role in determining the dye's quenching efficiency, the fluorescence of PPESO3 was quenched with the cyanine dye trication, Cy^{3+} (Scheme 1). Figure 2b compares the SV quenching plots for Cy^{3+} and HMIDC. The latter dye has similar absorption and fluorescence wavelengths compared to Cy^{3+}, but it only carries a +1 charge. Two features are readily apparent from the plots in Figure 2b. First, at very low concentrations (<200 nM) Cy^{3+} and HMIDC follow almost the same SV correlation; however, at higher dye concentration the plots diverge, showing that Cy^{3+} is a considerably more efficient quencher. It is also quite apparent that the Cy^{3+} SV plot features strong upward curvature.

In general, it is evident that Cy^{3+} is a more efficient quencher than the other cyanines. In part the enhanced quenching efficiency arises because the association constant for the Cy^{3+}-PPESO3 complex is larger compared to the other dyes. This is due to the increased electrostatic interaction, which is caused by the larger charge on Cy^{3+}. However, in addition to the stronger association constant, another effect contributes to the significantly enhanced quenching efficiency: dye-induced aggregation of the polymer chains. As the concentration of Cy^{3+} increases, the dye acts to bridge polyanion chains, inducing formation of polymer aggregates. Quenching is enhanced significantly because, within the Cy^{3+}-polymer aggregates interchain exciton migration occurs, effectively increasing the dye's quenching sphere of action. In effect, dye-induced polymer aggregation turns on pathways for three-dimensional exciton migration, and the enhanced dimensionality of exciton migration in the aggregates significantly increases the quenching efficiency of the dye.[50−52] The fact that the dye induces polymer aggregation is evidenced by the quenching data, as the Cy^{3+} quencher shows a $[Q]_{90}$ value that is considerably less than that for the monovalent quenchers, which reflects the fact that the quenching efficiency is amplified more as the Cy^{3+} concentration increases. Evidence for Cy^{3+}-induced aggregation of PPESO3 also comes from absorption spectroscopy. In particular, as the dye is added to the methanol solution of polymer, the polymer's absorption shifts from 425 to 445 nm (see Figure S3 in Supporting Information). The dye-induced shift in absorption is similar to that seen when polymer aggregation is induced by changing the solvent from methanol to water.

The trivalent dye induces aggregation of the PPESO3 chains in accordance with the typical behavior of polyelectrolytes in the presence of polyvalent counterions.[53,54] In addition, in previous work we presented evidence that the addition of a divalent quencher (MV^{2+}) to a methanol solution of PPESO3 caused changes in the absorption and fluorescence spectra consistent with the formation of the aggregated state of the polymer.[5] Polyvalent ionic quenchers have also been suggested to induce aggregation of the PPV-type conjugated polyelectrolyte MPS-PPV.[4,16,22]

PPESO3 Induced Aggregation of HMIDC. While the optical properties of mixtures of PPESO3 with the cyanines in various solvents were investigated, evidence was uncovered indicating that under certain conditions the conjugated polymer can template the formation of cyanine aggregates. Cyanines are known to have a propensity to aggregate in water, even at very low concentrations.[55] Two general classes of cyanine dye aggregates are known: H-aggregates (face-to-face stacking), which are characterized by a blue-shifted absorption and weak photoluminescence, and J-aggregates (slipped stacking), which are characterized by red-shifted absorption and strong red-shifted fluorescence.[56] It has been shown that polyelectrolytes, colloids, and crystallites can induce the formation of H- and J-type aggregates of cyanine dyes.[57−61] Recent studies have demonstrated that DNA can template the formation of J-aggregates of cyanine dyes (by analogy to PPESO3, DNA is an anionic, rigid rod polyelectrolyte).[47,62]

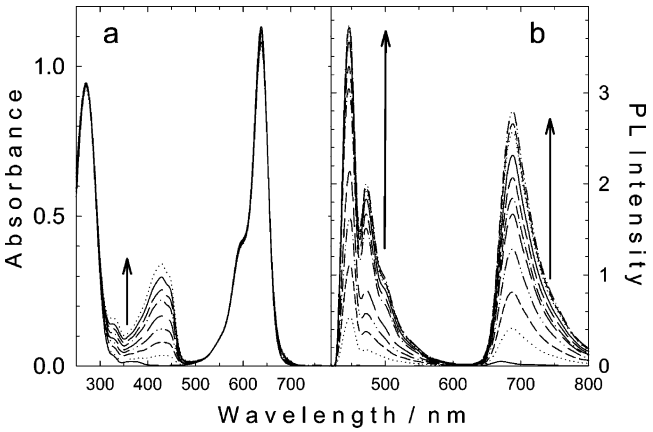

Figure 3. UV−visible absorption (a) and fluorescence (b) spectra of HMIDC (4.9 μM) in CH_3OH during titration with PPESO3. Fluorescence emission spectra were measured with excitation wavelength at 400 nm. PPESO3 was added in 0.5 μM aliquots, giving a total concentration range from 0 to 4 μM.

Figure 3a illustrates the absorption spectra of a solution of HMIDC (4.9 μM) in CH_3OH titrated with PPESO3 (0−4 μM). At the outset of the titration, the solution contains only HMIDC, which has absorption bands at 275 and 636 nm. As PPESO3 is added to the CH_3OH solution, the polymer's absorption at 425 nm grows in, but no other change is seen in the spectrum. Figure 3b illustrates the changes that are observed in the fluorescence spectrum (with excitation at 400 nm, corresponding to PPESO3 absorption) concomitant with titration of PPESO3 into the HMIDC solution. At the outset of the experiment, only HMIDC is present in the solution, and since the dye's absorbance at 400 nm is very weak, little fluorescence is measured. However, as PPESO3 is added, two fluorescence bands with increasing intensity are observed. The first at $\lambda_{max} = 450$ nm corresponds to fluorescence from PPESO3. (This fluorescence is considerably weaker than that of a solution containing only PPESO3

(50) Baumann, J.; Fayer, M. D. *J. Chem. Phys.* **1986**, *85*, 4087−4107.
(51) Levitsky, I. A.; Kim, J.; Swager, T. M. *J. Am. Chem. Soc.* **1999**, *121*, 1466−1472.
(52) Beljonne, D.; Pourtois, G.; Silva, C.; Hennebicq, E.; Herz, L. M.; Friend, R. H.; Scholes, G. D.; Setayesh, S.; Mullen, K.; Bredas, J. L. *Proc. Natl. Acad. Sci. U.S.A.* **2002**, *99*, 10982−10987.
(53) Grønbech-Jensen, N.; Mashl, R. J.; Bruinsma, R. F.; Gelbart, W. M. *Phys. Rev. Lett.* **1997**, *78*, 2477−2480.
(54) Khan, M. O.; Mel'nikov, S. M.; Jonsson, B. *Macromolecules* **1999**, *32*, 8836−8840.
(55) West, W.; Pearce, S. *J. Phys. Chem.* **1965**, *69*, 1894−1903.
(56) Kasha, M.; Rawls, H. R.; El-Bayoumi, A. *Pure Appl. Chem.* **1965**, *11*, 371−393.
(57) Herz, A. In *The Theory of the Photographic Process*; McMillan: New York, 1977.
(58) Horng, M.-L.; Quitevis, E. L. *J. Phys. Chem.* **1993**, *97*, 12408−12415.
(59) Ogawa, M.; Kawai, R.; Kuroda, K. *J. Phys. Chem.* **1996**, *100*, 16218−16221.
(60) Place, I.; Perlstein, J.; Penner, T. L.; Whitten, D. G. *Langmuir* **2000**, *16*, 9042−9048.
(61) Peyratout, C.; Donath, E.; Daehne, L. *J. Photochem. Photobiol. A* **2001**, *142*, 51−57.
(62) Seifert, J. L.; Connor, R. E.; Kushon, S. A.; Wang, M.; Armitage, B. A. *J. Am. Chem. Soc.* **1999**, *121*, 2987−2995.

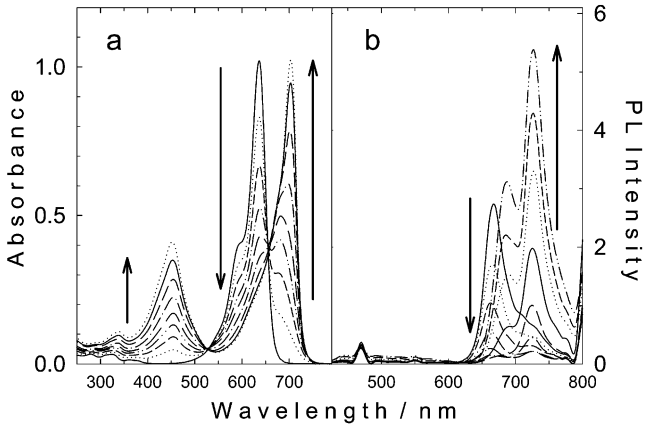

Figure 4. UV−visible absorption (a) and fluorescence (b) spectra of HMIDC (4.9 μM) in water during titration with PPESO3. Fluorescence emission spectra were measured with excitation wavelength at 400 nm. PPESO3 was added in 0.5 μM aliquots, giving a total concentration range from 0 to 5 μM.

because of quenching by HMIDC.) More interesting is the appearance of a second band corresponding to fluorescence from HMIDC (λ = 685 nm) and the fact that the fluorescence intensity increases with increasing PPESO3 concentration. This observation clearly indicates that energy transfer occurs from PPESO3 to HMIDC and that the sensitized fluorescence emanates from the PPESO3−HMIDC ion-pair complex. The maximum and band shape of the HMIDC fluorescence from the complex are similar to those observed for the free dye in CH_3OH solution. However, the fluorescence is slightly red-shifted (relative to that for the uncomplexed dye), which indicates that the dye excited state is stabilized by interaction with the polymer.

Figure 4 panels a and b illustrate, respectively, the absorption and fluorescence spectra of HMIDC (4.9 μM) in H_2O during titration with PPESO3 (0−5 μM). As seen in Figure 4a, addition of PPESO3 to the aqueous dye solution induces significant changes in the dye's absorption. In particular, at the outset of the titration, the dye's absorption appears at λ_{max} = 635 nm. As PPESO3 is added, the 635 nm absorption decreases, and it is replaced by a red-shifted absorption in the 680−700 nm region. Close inspection of the new absorption band shows that although there is an isosbestic point maintained during the addition of PPESO3, the λ_{max} of the red-shifted band is not constant. The changes in fluorescence of HMIDC upon addition of PPESO3 are shown in Figure 4b (in these experiments excitation is at 400 nm). As the PPESO3 is added to the aqueous solution of HMIDC, the fluorescence of the free dye decreases (λ_{em} = 667 nm), and it is replaced by a red-shifted fluorescence that appears as two bands, at λ_{max} = 686 and 726 nm. (Note that in water the fluorescence of PPESO3 is entirely quenched by the HMIDC. In general, it is seen that quenching is more efficient when the polymer is aggregated.[5])

Taken together, the results indicate that HMIDC complexes with PPESO3 in CH_3OH, but the polymer-complexed dye is not in an aggregated form. By contrast, the spectroscopic observations on the same system in water suggest that, in the dye−polymer complex, the dye exists as a J-aggregate. This premise is supported by the fact that the absorption and fluorescence of the PPESO3−HMIDC complex are both red-shifted significantly from those of the monomer. In addition, the fluorescence band that appears from the complex at λ_{max} = 726 nm is relatively narrow in bandwidth and is consistent with emission from a J-aggregate of the cyanine dye.[56]

Table 2. Parameters Recovered from Kinetic Modeling of PPESO3 Fluorescence Decays with HMIDC in Methanol[a]

[HMIDC]/μM	[PRU]:[dye]	F_q[b]	A_r	τ_0/ps	β_0	τ_2/ps	β_2
0		1	1	150	0.6		
0.4	85:1	0.5	0.2	150	0.6	1500	0.25
1.2	28:1	0.75	0.41	150	0.6	760	0.25
5.0	6.8:1	0.93	0.64	150	0.6	20	0.2

[a] [PPESO3] = 34 μM in CH_3OH. [b] Fraction of total PPESO3 fluorescence quenched ($F_q = 1 - I/I^0$, where I and I^0 are, respectively, the PPESO3 fluorescence intensity with and without added HMIDC quencher).

An important question relates to the structure of the HMIDC J-aggregate that is templated by PPESO3. Any model for the structure of the dye aggregate must take into account that the polymer is aggregated in H_2O. As shown in Scheme 2, in water the aggregated PPESO3 chains are stacked, with the ionic sulfonate groups extending into the polar solvent.[63] The PPESO3 aggregate presents a polar/ionic face to the solvent environment, and the HMIDC dye molecules adsorb to this face in order to maximize ion-pair interactions with the polymer and minimize hydrophobic interactions between the dye and the aqueous solvent. Apparently the dyes adsorb in an ordered arrangement on the face such that the J-aggregate is formed (Scheme 2). Molecular modeling indicates that the length of an HMIDC molecule (16 Å) exceeds that of a single PPESO3 repeat unit (12 Å). Therefore, to allow the maximum number of HMIDC molecules to associate with the stacked polymer chains, the dyes orient such that their long axis is offset relative to the long axis of the polymer chains in the stacked array. This effect leads to the necessary condition for J-aggregate formation—the dyes are oriented in a slipped stack which produces the interchromophore orientation characteristic of the J-aggregate.

Time-Resolved Fluorescence Spectroscopy. To further investigate the mechanism of PPESO3-to-cyanine energy transfer, we carried out picosecond time-resolved fluorescence experiments by using fluorescence upconversion. These experiments were carried out at a fixed PPESO3 concentration (34 μM). HMIDC was selected as the acceptor cyanine dye, and its concentration was varied from 0 to 5 μM. Concomitant with the time-resolved experiments, parallel steady-state quenching measurements were carried out, and the fraction of the quenched PPESO3 fluorescence ($F_q = 1 - I/I^0$) for the PPESO3/HMIDC solutions are listed together with the time-resolved data in Table 2. All of the time-resolved experiments were carried out in methanol solution to minimize the influence of polymer aggregation on the observed fluorescence dynamics.

By using a laser excitation wavelength of 425 nm, it is possible to directly excite PPESO3 (see Figure 3a). HMIDC was selected as the energy acceptor for these studies because it absorbs only very weakly at 425 nm, and consequently when a 425 nm wavelength is used to excite the PPESO3/HMIDC mixtures, excitations localized on HMIDC are created almost exclusively by energy transfer from the polymer. In addition, owing to the large wavelength separation between the fluorescence of PPESO3 ($\lambda \approx$ 450 nm) and HMIDC ($\lambda \approx$ 685 nm), it

(63) If this model for the PPESO3 aggregate is correct, the ionic face of the aggregate is very similar to the surface of an ionic material, for example, a clay surface or silver halide crystal. Such ionic surfaces are known to template the formation of J-aggregates, see refs 51 and 53.

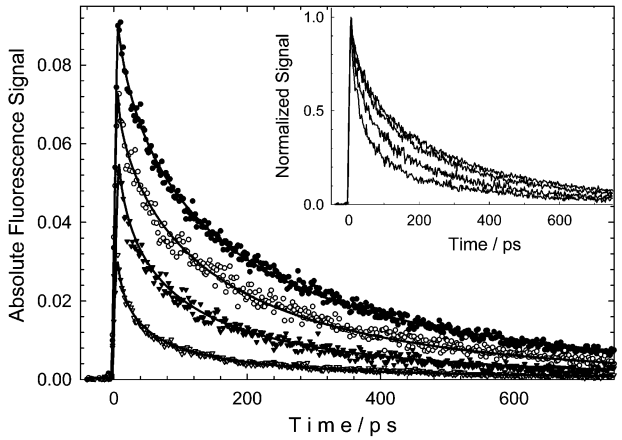

Figure 5. Absolute fluorescence decays of PPESO3 (34 μM) in CH_3OH with and without HMIDC quencher. Fluorescence emission spectra were measured with excitation wavelength at 425 nm and detection at 450 nm. Symbols represent experimental data, and solid lines are calculated from eq 4 along with the parameters listed in Table 2. In order of decreasing initial intensity: PPESO3 only, PPESO3 + 0.4 μM HMIDC ($F_q = 0.5$); PPESO3 + 1.2 μM HMIDC ($F_q = 0.75$); PPESO3 + 5.0 μM HMIDC ($F_q = 0.93$). The inset shows the same decay data in a normalized format.

is possible to selectively observe the fluorescence dynamics for PPESO3 and HMIDC (the energy donor and acceptor, respectively).

Figure 5 shows fluorescence decays detected at 450 nm with 425 nm excitation for a series of solutions that contain PPESO3 and HMIDC at concentrations ranging from 0 to 5 μM. The decay curves that are plotted in Figure 5 represent absolute fluorescence intensities, since they were obtained under identical conditions (matched solution concentrations of PPESO3, identical pump power and detection settings). Therefore, the amplitudes of the decays reflect the true relative instantaneous intensity of the time-resolved fluorescence signal from the different samples. Upon inspection of the data, two features are apparent. First, the initial amplitude of the polymer's fluorescence decay is reduced by the addition of HMIDC. Second, with increasing HMIDC concentration, the fluorescence decays more rapidly, which can be better seen in the inset of Figure 5, where normalized data are plotted. Taken together, these observations indicate that the PPESO3-to-HMIDC energy transfer takes place on two distinct time scales. A significant component of the transfer occurs by a pathway that is so fast that it cannot be resolved within the instrument response ($\sim$4 ps). In addition, the clearly noticeable increase in the rate of the fluorescence decay with increasing HMIDC concentration (see inset, Figure 5) indicates that there is also a slow energy transfer process, which may represent diffusion of the exciton to the HMIDC acceptor.

To model the decay kinetics of the PPESO3 fluorescence, in both the absence and presence of the HMIDC quencher, a stretched exponential function of the form

$$I(t) = (1 - A_r) \exp[-t/\tau_0]^{\beta_0} \exp[-t/\tau_2]^{\beta_2} \qquad (4)$$

was used. In eq 4, $I(t)$ represents the fluorescence intensity at time t, the parameters τ_0 and β_0 model the natural decay kinetics of the polymer, and τ_2 and β_2 model the dynamics of the slow energy transfer pathway. The β terms provide a measure of the width of the lifetime distribution ($0 < \beta \leq 1$, where the width of the distribution increases as β decreases). The term appearing in the preexponential, A_r, accounts for the reduction in the initial amplitude of the fluorescence due to the prompt quenching pathway (lifetime $\tau_1 < 4$ ps).

The fluorescence decay of PPESO3 in the absence of HMIDC is fitted by eq 4 with the decay time $\tau_0 = 150$ ps and $\beta_0 = 0.6$ ($\tau_2 = \infty$) The observation of a stretched exponential decay for the polymer's fluorescence is not surprising in view of the fact that there is heterogeneity in the chromophores within the polymer chains (for example, due to a distribution of conjugation lengths caused by rotation around the Ph$-$C$\equiv$C bonds). In addition, studies of the fluorescence decay characteristics of phenylene ethynylene oligomers reveal complex dynamics on the 0$-$100 ps time scale associated with solvation and conformational relaxation of the initially produced singlet exciton.[64] It is likely that similar processes occur in the polymer.

The decays obtained for solutions that contain HMIDC were fitted also by use of eq 4, with τ_0 and β_0 held constant and allowing variation of A_r (the amplitude of the prompt quenching pathway), τ_2, and β_2 (the lifetime and distribution width of the slow energy transfer pathway). The parameters recovered from the fits are collected in Table 2, and several trends are evident from these data. First, the amplitude of the prompt process (A_r) increases significantly with increasing HMIDC concentration. Comparison of the value of A_r with the fraction of total emission quenched (F_q) reveals that, on average, the prompt energy transfer process accounts for more than half of the total fluorescence quenching. This clearly demonstrates that a substantial component of the PPESO3-to-HMIDC energy transfer takes place on an ultrafast time scale (i.e., $\tau < 4$ ps). In addition to the ultrafast quenching pathway, the fits reveal that a second, slower energy transfer pathway is operative (τ_2 and β_2, Table 2). The time constant of this slow pathway decreases substantially with increasing HMIDC concentration, yet in all cases the lifetime distribution is broad as reflected by the fact that β_2 is low (0.2$-$0.25).

The notion of energy transfer being active on two distinct time scales is confirmed by the temporal behavior of the HMIDC fluorescence. Figure 6 compares the rise and decay kinetics of the HMIDC fluorescence for three different samples. First, excitation of a CH_3OH solution of pure HMIDC, with $\lambda_{ex} = 636$ nm and $\lambda_{em} = 663$ nm (at the maximum of the pure-dye emission), produces a fluorescence signal that rises within the instrument response and decays with $\tau = 285$ ps (single exponential). This is the natural lifetime of HMIDC in CH_3OH solution. Next, decays were obtained for mixtures of PPESO3 (34 μM) and HMIDC (1.2 and 5.0 μM). In this case the solutions were excited at 425 nm (PPESO3 absorption) with the HMIDC fluorescence detected at 685 nm. It is evident that, for both solutions containing PPESO3, the decay rate of the HMIDC fluorescence ($\tau \approx 1.2$ ns) is slower compared to that of the pure HMIDC solution. The slower decay rate is believed to arise from stabilization of the excited state of the dye upon complex formation with the PPESO3 chain. Of more interest is that, for both solutions containing PPESO3 and HMIDC, the rise of the dye's fluorescence features two distinct components. The majority of the HMIDC fluorescence signal rises with an instrument-limited response ($\tau_1 < 4$ ps), confirming that a

(64) Sluch, M. I.; Godt, A.; Bunz, U. H. F.; Berg, M. A. *J. Am. Chem. Soc.* **2001**, *123*, 6447$-$6448.

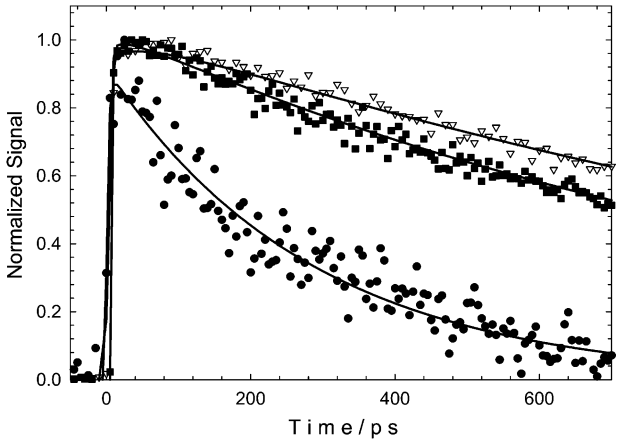

Figure 6. Time-resolved fluorescence of HMIDC in CH_3OH with and without PPESO3. The symbols represent the experimental data, and solid lines are calculated as described in the text. (●) HMIDC only (7 μM), λ_{ex} = 636 nm, λ_{em} = 663 nm. (▽) PPESO3 (34 μM) + HMIDC (1.3 μM, F_q = 0.75), λ_{ex} = 425 nm, λ_{em} = 685 nm). (■) PPESO3 (34 μM) + HMIDC (5 μM, F_q = 0.93), λ_{ex} = 425 nm, λ_{em} = 685 nm.

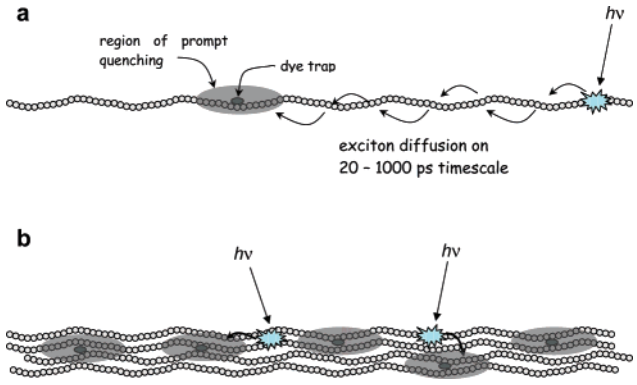

Figure 7. Cartoon depicting the processes involved in quenching of the PPESO3 exciton by complexed dye. (a) High polymer:dye concentration ratio, unaggregated polymer chain. The gray ellipse represents the prompt quenching region. In this situation some excitons are quenched rapidly and others more slowly due to the requirement for exciton diffusion along the chain. (b) Low polymer:dye concentration ratio, aggregated polymer. In this situation all excitons are in close proximity to the quenching region and quenching is dominated by rapid processes involving intra- and interchain exciton diffusion.

significant component of the PPESO3 to HMIDC energy transfer occurs on an ultrafast time scale. However, in addition to the prompt rise component, both solutions exhibit a clearly resolved slow rise-time component, which corresponds to the slow energy transfer process resolved in the PPESO3 fluorescence decay experiments described earlier (characterized by τ_2 and β_2). The solid lines shown in Figure 6 were generated by using the same kinetic parameters used to fit the PPESO3 decays (Table 2), which reinforces the hypothesis that the effect of HMIDC on PPESO3 fluorescence decay dynamics corresponds to an energy transfer process.

Model for Energy Transfer in PPESO3−Cyanine Ion-Pair Complexes. The steady-state and time-resolved fluorescence experiments described above provide clear evidence that energy transfer quenching in the PPESO3−cyanine complexes occurs on two time scales: one occurring within the temporal response of the upconversion experiments (τ_1 < 4 ps, k_1 > 0.25 ps^{-1}) and a second that has a rate comparable to the natural decay rate of the singlet exciton ($\tau_2 \approx 20-1000$ ps, $k_2 \approx 0.05-0.001$ ps^{-1}). In this section we discuss the origin of two PPESO3-to-HMIDC energy transfer pathways.

First, consider the ground-state and excited-state structure of PPESO3. One polymer repeat unit (PRU) consists of two phenylene ethynylene moieties (every other phenylene ring is functionalized with alkoxysulfonate side groups). Molecular modeling indicates that a PRU is ∼1.2 nm in length. On average, a PPESO3 chain consists of ∼100 PRUs,[5] and therefore an average chain is ∼120 nm in length. This distance is large compared to the Förster radii of the dye quenchers (R_0 = 4.9 nm for HMIDC). As shown by the steady-state spectroscopy, the phenylene ethynylene linkages are not rigid, consequently in CH_3OH (a good solvent) the chains are expected to exist in more-or-less extended conformations,[65,66] and therefore it is unlikely that regions of the polymer separated by many PRUs are in close spatial proximity. Excitation of PPESO3 rapidly affords the singlet exciton (^1B_u) that is responsible for the polymer's strong fluorescence. Studies of model phenylene ethynylene oligomers reveal that the relaxed ^1B_u exciton is delocalized over approximately 10−12 phenylene ethynylene repeats (this corresponds to 5−6 PPESO3 PRUs).[67−69] However, because in the ground state there is little barrier to rotation of the phenylene units around the polymer long axis, there is a broad distribution of segments with differing conjugation lengths, and consequently initial photoexcitation likely produces a distribution of excitons having different conjugation lengths. Conformational relaxation of the exciton via rotation of the phenylenes into an all-planar geometry is believed to occur with $\tau \approx 60$ ps ($k \approx 0.02$ ps^{-1}).[64]

The time-resolved measurements were carried out with solutions that contain a stoichiometric excess of PPESO3 PRUs. At the highest dilution (HMIDC = 0.4 μM), the PRU:HMIDC ratio is 85:1; assuming that all of the HMIDC is complexed to the polymer,[70] the solution will consist mainly of PPESO3 chains with one dye complex (along with a fraction of chains with no dyes complexed, and a small fraction with two or more dye complexes). The surprising feature is that even at 1 dye complex/chain, a substantial fraction (∼0.20) of the total emission is quenched promptly (i.e., within 4 ps). This ultrafast energy transfer pathway is rationalized as follows. Considering a Förster radius of 50 Å, and τ = 150 ps, and assuming that Coulombic interactions are the predominant mechanism for the polymer−dye energy transfer, we estimate that polymer-based excitons within 27 Å of an HMIDC acceptor (∼2 PRUs on either side of the dye binding site) will be quenched within 4 ps after excitation. The range of prompt quenching is augmented by exciton delocalization.[67−69] Given that the delocalization length of the PPESO3 exciton is 5 PRUs, then an exciton produced within a radius consisting of ∼14 PRUs (7 PRUs on either side of the dye binding site, ca. 14% of an average polymer chain; see Figure 7a) will be quenched within 4 ps. Interestingly, the fraction of a typical polymer chain that is

(65) Cotts, P. M.; Swager, T. M.; Zhou, Q. *Macromolecules* **1996**, *29*, 7323−7328.
(66) Liu, J. F.; Ducker, W. A. *Langmuir* **2000**, *16*, 3467−3473.
(67) Ziener, U.; Godt, A. *J. Org. Chem.* **1997**, *62*, 6137−6143.
(68) Jones, L., II; Schumm, J. S.; Tour, J. M. *J. Org. Chem.* **1997**, *62*, 1388−1410.
(69) Kukula, H.; Veit, S.; Godt, A. *Eur. J. Org. Chem.* **1999**, 277−286.
(70) Calculations with $K_{assoc} = K_{SV} = 1.1 \times 10^6$ M^{-1} indicate that at the polymer and dye concentrations used in the time-resolved experiments the majority of the dye is complexed to the polymer.

covered by the prompt quenching radius (~0.14) corresponds approximately to the fraction of the emission that is quenched instantaneously (0.2) in the solution that contains 85:1 PRU:dye. The fraction of the fluorescence promptly quenched increases as the dye concentration increases. This is because as the PRU:dye stoichiometry decreases, more than a single dye is complexed to each polymer chain, and consequently the fraction of excitons produced on a chain within the prompt quenching radius of a dye binding site increases considerably.

Now we consider the origin of the slow energy transfer pathway (τ_2, Table 2). This process is believed to arise primarily from intrachain diffusion of a singlet exciton, which is initially produced on a polymer chain at a site distant from the prompt quenching radius of the dye-binding site. The event involves a random walk of the exciton along the polymer via a sequence of intrachain hops mediated by Coulombic interactions between adjacent (or nearby) chromophore segments (see Figure 7a).[52] The dynamics of this process accelerate with increasing dye concentration, because the average distance between the exciton and the nearest dye decreases, decreasing the overall transfer time. In support of this model, we note that a recent experimental and theoretical investigation of intrachain energy transfer in a perylene end-capped poly(indenofluorene) indicated that the dynamics of intrachain singlet exciton diffusion take place on the 0.1−1 ns time scale.[52] The experimental observations and simulations described in this work are in direct agreement with the model that we use to interpret the fluorescence dynamics in the PPESO3−HMIDC system.

Finally, it is useful to consider the relationship between the steady-state and time-resolved quenching data because it provides insight into the mechanism for amplified quenching, which is key to the sensor application of CPEs.[4,23,26] Extrapolation of the steady-state SV plots to very low quencher concentration (<100 nM) reveals a region that is approximately linear. The time-resolved experiments show that at these low quencher concentrations the excited-state lifetime of the PPESO3 is not affected; hence the dynamics are dominated by the prompt component. Thus, we conclude that, at very low quencher concentration, quenching is dominated by a traditional static model (eq 2, where $K_{SV} \approx K_a$), wherein the dominant mode of quenching results from excitons that are produced on a polymer chain within the prompt quenching volume of a dye quencher (i.e., an exciton produced in the dark region around the dye in Figure 7a). In this quenching domain, large K_{SV} values arise because the association constant between the polymer chain and the dye is large, and the prompt quenching volume includes 15 or more PRUs. As the quencher concentration increases, the SV plots display upward curvature, indicating that additional quenching pathways become important. At least two additional pathways can be identified. First, as the number of dyes bound per chain increases, the probability increases for an exciton produced outside of a prompt quenching radius to be quenched by diffusion to the dye complex site. This process leads to a faster PPESO3 emission decay as seen in the time-resolved experiments (i.e., dynamic quenching becomes important). Second, as noted above, at higher dye concentration polymer aggregation occurs (especially with polyvalent quencher ions), and the possibility of interchain diffusion of excitons becomes significant (see Figure 7b). Polymer aggregation significantly increases the probability that an exciton will be produced within close proximity to a bound dye, increasing the contributions of prompt and diffusional quenching to the overall quenching. Similar conclusions regarding the importance of polymer aggregates in promoting amplified quenching were drawn in studies of MPS-PPV.[4,5,22]

Summary and Conclusions

This investigation examined fluorescence quenching of the anionic conjugated polyelectrolyte PPESO3 with a series of cationic cyanine dyes toward the objective of providing insight into the mechanism of amplified quenching. Quenching involves energy transfer from the polymer (energy donor) to the dyes (energy acceptor), as confirmed by the observation of sensitized fluorescence from the dyes. Steady-state and time-resolved fluorescence experiments carried out under conditions where the polymer is not strongly aggregated reveal that quenching is dominated by an ultrafast energy transfer pathway believed to arise when a polymer-based exciton is produced within a Förster capture radius of the complexed dye. A slower quenching pathway that becomes significant at higher dye concentrations is believed to arise from intrachain exciton diffusion along a conjugated polymer chain. Evidence is also presented indicating that, in solvents where the conjugated polymer is aggregated, the aggregate can function as a template for the formation of cyanine dye J-aggregates.

Taken together, the work presented herein provides insight into approaches that can be taken to optimize CPE-based chemo- and biosensors.[4,23,26] Amplified quenching is clearly enhanced in systems in which the conjugated polyelectrolytes are aggregated. This takes advantage of the fact that the effective capture radius of the quencher is increased due to intra- and interchain exciton diffusion in the aggregates. In addition, polyvalent quenchers are preferred because these species have larger association constants for binding to the polyelectrolyte and also because they will increase the probability for formation of interchain aggregates near the binding site of the dye.

Acknowledgment. We gratefully acknowledge the United States Department of Energy, Office of Basic Energy Sciences (DE-FG-02-96ER14617) for support of this work.

Supporting Information Available: Figures showing the viscosity of PPESO3 solutions, the fluorescence of PPESO3 and the absorption of DOC, DODC, and DOTC in methanol solution, and the effect of Cy^{3+} on the absorption of PPESO3 in methanol. This material is available free of charge via the Internet at http://pubs.acs.org.

JA046856B